Optimization of constant-length Rowland-circle monochromator with a varied line-spacing grating

Lijun Lu (吕丽军)

Fine Mechanical Engineering Department, Shanghai University, Shanghai 200074

Received February 10, 2004

We use a varied line-spacing (VLS) grating to improve the performances of the constant-length Rowland-circle spherical grating monochromator. The translation distance of the mirror-grating tank in a scan of certain wavelength range will get much shorter. This will make the instrument easier to realize. Based on the principle of monochromator, we study how to optimize the optical system with a VLS grating in detail. The main imaging performances of the instrument are also evaluated.

OCIS codes: 340.6720, 120.6200, 050.1950.

The constant-length Rowland-circle spherical grating monochromator was first presented by Ishiguro[1], and further developed by Senf *et al.*[2]. This spherical grating monochromator can keep the position of slits and light beam direction fixed; besides it almost satisfies the Rowland-circle condition in the working wavelength range. But a scan of wavelength range such as 1.24−3.24 nm requires the mirror-grating tank to move as long as above 1 m. Such a long mechanical track easily gets curved because of the variation of temperature and the heavy load of the whole vacuum chamber. On the other hand, the positioning accuracy of optical elements needs to keep below 1 μrad to attain a resolving power of as high as 10000. Thus the scanning mechanism of the monochromator is very difficult to realize[3]. The proposed design is to use a varied line-spacing (VLS) grating[4−6] instead of a conventional one in the constant-length spherical grating monochromator to reduce the distance of translation of mirror-grating tank from above 1 m to 20−32.5 cm.

The optical system of the discussed monochromator is shown in Fig. 1. It consists of a plane pre-mirror and a VLS spherical grating. A wavelength scan is made by rotation of grating and translation of the mirror-grating tank. The plane mirror only plays a role of deflecting rays. So we only need to analyze the imaging of a VLS spherical grating itself.

To analyze the aberration of a grating system, the optical path function is a very useful tool. Figure 2 shows a scheme of a ray from a point source, A, diffracted by a VLS grating, and hitting a point B on the image plane.

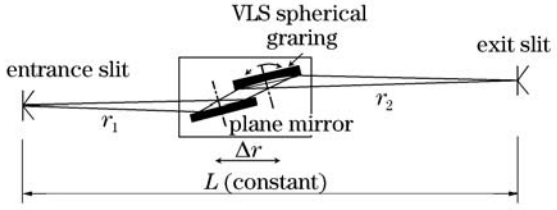

Fig. 1. The optical system of the monochromator. r_1 and r_2 are the distances from the grating to the entrance slit and to the exit slit, respectively; Δr is the translation distance required to scan a wavelength range.

The optical path function of a grating is defined by

$$F = \langle AP\rangle + \langle PB\rangle + Nm\lambda, \tag{1}$$

where $\langle AP\rangle$ and $\langle PB\rangle$ are the distances from a point on grating, $P(\xi,\omega,l)$, to source point A and to its image B; N, m, and λ are the number of grooves from the origin O to P, the diffraction order of grating, and the working wavelength, respectively. The groove spacing of a VLS grating can be assumed to have the following polynomial form,

$$d(w) = d_0(1 + b_2 w + b_3 w^2 + b_4 w^3 + \cdots). \tag{2}$$

The light path function of a VLS grating had been derived as[5,6]

$$F = F_{00} + wF_{10} + \frac{1}{2}w^2F_{20} + \frac{1}{2}l^2F_{02} + \frac{1}{2}w^3F_{30} + \frac{1}{2}wl^2F_{12} + \frac{1}{8}w^4F_{40} + \cdots. \tag{3}$$

Several important aberration coefficients F_{ij} in the dispersion plane are given by

$$\begin{aligned}
F_{10} &= -(\sin\alpha + \sin\beta) + \frac{m\lambda}{d_0},\\
F_{20} &= \left(\frac{\cos^2\alpha}{r_1} + \frac{\cos^2\beta}{r_2} - \frac{\cos\alpha + \cos\beta}{R}\right) - b_2\frac{m\lambda}{d_0},\\
F_{30} &= \left(\frac{\sin\alpha}{r_1}T(r_1,\alpha) + \frac{\sin\beta}{r_2}T(r_2,\beta)\right)\\
&\quad + \frac{2}{3}(b_2^2 - b_3)\frac{m\lambda}{d_0},\\
F_{40} &= \frac{4\sin^2\alpha}{r_1}T(\alpha,r_1) - \frac{T^2(\alpha,r_1)}{r_1}\\
&\quad + \frac{4\sin^2\beta}{r_2}T(\beta,r_2) - \frac{T^2(\beta,r_2)}{r_2} - \frac{\cos\alpha + \cos\beta}{R^3}\\
&\quad + \frac{1}{R^2}\left(\frac{1}{r_1} + \frac{1}{r_2}\right) - 2(b_2^3 - 2b_2b_3 + b_4)\frac{m\lambda}{d_0},
\end{aligned} \tag{4}$$

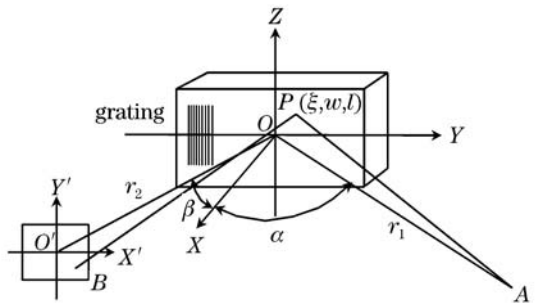

Fig. 2. Ray from a source point A, diffracted by a VLS grating, hits the image plane at point B. α and β are the angles of incidence and diffraction of grating; r_1 and r_2 are the entrance- and exit-arm lengths.

where $T(r,\alpha) = \left(\cos^2\alpha/r\right) - \cos\alpha/R$; R is the radius of grating; F_{20}, F_{30}, and F_{40} are coefficients of defocus, coma, and spherical aberration, respectively.

To a soft X-ray monochromator, first of all we try to make the defocus term be zero, which leads to the focusing equation

$$\left(\frac{\cos^2\alpha}{r_1} + \frac{\cos^2\beta}{r_2} - \frac{\cos\alpha + \cos\beta}{R}\right) - b_2\frac{m\lambda}{d_0} = 0. \quad (5)$$

On the other hand, a grating system must satisfy $F_{10} = 0$, which directly leads to the grating equation

$$d_0(\sin\alpha + \sin\beta) = m\lambda. \quad (6)$$

Under the boundary condition of the monochromator we find that the solution of Eqs. (5) and (6) could lead to a much smaller value of Δr by properly selecting the value of b_2.

The solution of Eqs. (5) and (6) can be solved only numerically. For comparison we use the monochromator parameters as in Ref. [2]: the total length of the monochromator $L = 8$ m, a constant included angle of 174°, a spherical grating with groove density of 1000 lines/mm to work in the wavelength range of 1.24–3.24 nm. We can calculate the distribution of r_2 with wavelength if b_2 and R separately take specific values. The numerical results are shown as Figs. 3 and 4. We find that the parameters b_2 and R have different effects on the distribution of r_2. The value of b_2 basically determines the overall scale of r_2; the value of R causes a big variation of r_2 toward short wavelength end. For each b_2, we could find a specific value of R to make variation range of r_2, Δr, get to a minimum when the values of r_2 at the lower and upper ends of wavelength range are equal. For example, R is found to be 84.80 m if $b_2 = 1.1\times10^{-4}$ mm^{-1}.

Secondly, there exists a specific lower limit of b_2 that makes Eqs. (5) and (6) solvable at all wavelengths. With the above monochromator parameters, the value of the lower limit of b_2 will be 1.1×10^{-4} mm^{-1} (we take two effective digits of b_2). Figure 4 shows the distribution of the exit-arm length for different values of b_2 from 1.1×10^{-4} to 3.0×10^{-4} mm^{-1}. The overall scale of r_2 drops down and Δr gets smaller with the increase of b_2. The value of Δr ranges between 10–32.5 cm. It is much smaller compared with 1.4 m in Senf's design[2].

Besides the factor of Δr, we need to study how b_2 affects optical imaging of the monochromator. The main remaining aberrations in the dispersion plane are coma and spherical aberrations. Figures 5 and 6 show the coma and spherical aberration limited resolution of the monochromator system. In the calculations the vertical acceptance angle of the monochromator to the incident beam is set to be 0.8 mrad. The value of b_3 in Eq. (2) is determined in such a way that the coma aberration at the upper end of wavelength range is zero. Corresponding to the values of b_2 from 1.1×10^{-4} to 3.0×10^{-4} mm^{-1}, the resultant values of b_3 are from -4.9×10^{-8} to -8.2×10^{-8} mm^{-2}, respectively. The coma aberration is small enough for attaining a resolving power of 10000,

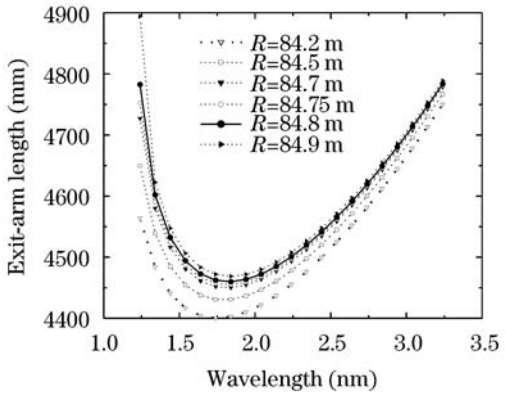

Fig. 3. The exit-arm length varies with wavelength for different values of R, $b_2 = 1.1\times10^{-4}$ mm^{-1}.

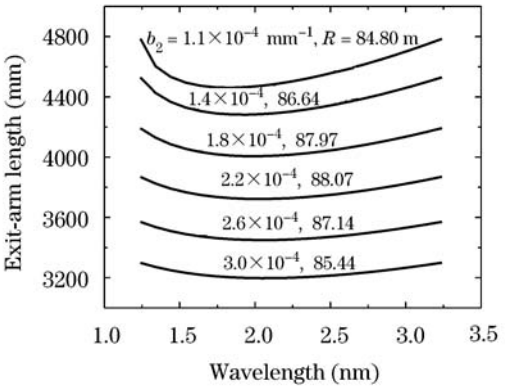

Fig. 4. The exit-arm length varies with wavelength for sets of (b_2, R).

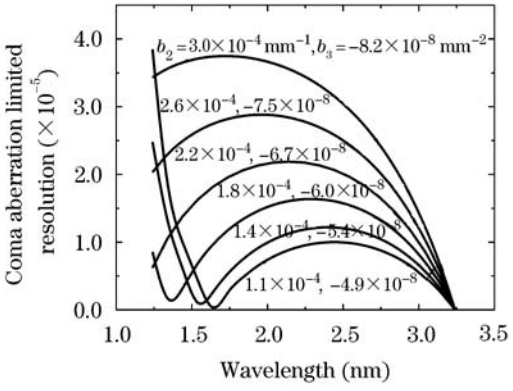

Fig. 5. Coma aberration limited resolutions are given for sets of (b_2, b_3).

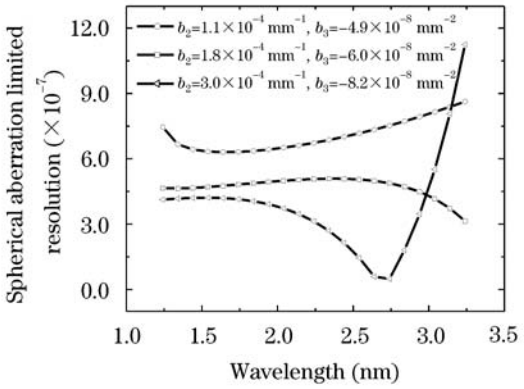

Fig. 6. Spherical aberration limited resolutions are given for sets of (b_2, b_3).

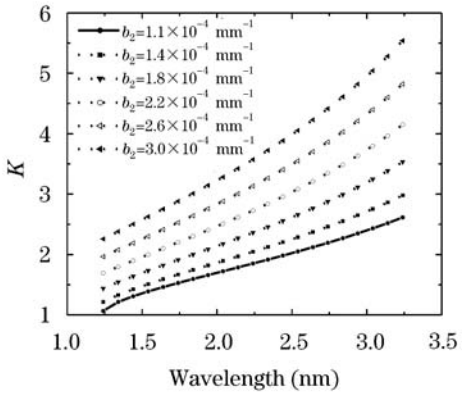

Fig. 7. The imaging demagnification K of the monochromator for the different values of b_2.

and the spherical aberration is negligible even without considering b_4 in Eq. (2). The aberration performances are quite good.

In the case of a synchrotron-radiation beamline, the demagnification ratio of monochromator ($K = r_1 \cos\beta / r_2 \cos\alpha$) will affect the design of pre-focusing and refocusing optics as well as the best matching between entrance- and exit-slit openings. Figure 7 shows that K increases with the increase of b_2 and wavelength; secondly, K deviates more strongly from 1 with the increase of b_2, so that the instrument does not satisfy Rowland-circle condition (i.e., $K = 1$) any more. However, the coma aberration can be controlled to be small enough by the optimization of b_3, as discussed above. The higher the value of K, the larger the divergence angle of the exit beam. This is unfavorable to the design of post-focusing optics, especially when synchrotron-radiation users require a small light spot at the sample position. Thus from this point of view we prefer a small value of b_2.

Based on the above discussions, b_2 is a very important parameter for the monochromator design. It is reasonable in the discussed example to take the value of b_2 between $(1.1-1.8)\times10^{-4}$ mm^{-1}; consequently Δr ranges between 20.0−32.5 cm. This will make the instrument much easier to realize.

L. Lu's e-mail address is lulijun63@hotmail.com.

References

1. E. Ishiguro, M. Suzui, J. Yamazaki, E. Nakamura, K. Sakai, O. Matsudo, N. Mizutani, F. Fukui, and M. Watanabe, Rev. Sci. Instrum. **60,** 2105 (1989).
2. F. Senf, F. Eggenstein, and W. Peatman, Rev. Sci. Instrum. **63,** 1326 (1992).
3. F. Senf, H. Lammert, U. Flechsig, T. Zeschke, and W. B. Peatman, Rev. Sci. Instrum. **66,** 2154 (1995).
4. M. C. Hettrick, S. Bowyer, R. F. Malina, C. Martin, and S. Mrowka, Appl. Opt. **24,** 1737 (1985).
5. M. Itou, T. Harada, and T. Kita, Appl. Opt. **28,** 146 (1989).
6. W. R. Mckinney, Rev. Sci. Instrum. **63,** 1410 (1992).